Oxidation of pentan-2-ol – Part I: Theoretical investigation on the decomposition and isomerization reactions of pentan-2-ol radicals

Junfeng Bai[1], Yuxiang Zhu[1], Chong-Wen Zhou[*1], Guillaume Dayma[2,3], Zeynep Serinyel[2,3], Philippe Dagaut[2]

[1]School of Energy and Power Engineering, Beihang University, Beijing 100191, PR China

[2]CNRS, Institut de Combustion, Aérothermique, Réactivité et Environnement 1C, Avenue de la recherche scientifique, 45071 Orléans cedex 2, France

[3]Université d'Orléans, 6 Avenue du Parc Floral, 45100 Orléans, France

Email: cwzhou@buaa.edu.cn

Abstract

Theoretical investigations on the kinetics of pentan-2-ol radical decomposition and isomerization reactions have been carried out in this work, together with the thermochemistry data calculations for important species involved in the reaction process. The B2PLYPD3/6-311++G(d,p) level of theory was used to optimize the geometries of all of the reactants, transition states, products and also the hindered rotor treatment for lower frequency modes. Single-point energies of all species are determined at the ROCCSD(T) level using the cc-PVQZ and cc-pVTZ which were extrapolated to the complete basis set limit (CBS). RRKM/Master Equation has been solved to calculate the pressure- and temperature-dependent rate coefficients for all channels in the pressure range of 0.01–100 atm over 300–2000 K. Pressure and temperature dependent branching fractions of key species produced from different pentan-2-ol radicals shows that 1- and 2-pentene are important bimolecular products. The kinetics and thermochemistry data for the title reactions has been used in the part II of this work for model development for pentan-2-ol oxidation.

Keywords: Pentan-2-ol; Ab initio calculation; Rate constant; Thermodynamics;

1. Introduction

The increasing worldwide demand for sustainable energy resources and environmental protection has brought more and more attention in the research of alternative clean fuels [1-5]. Alcohols have already been considered as sustainable fuel for decades [6, 7] and a large number of experimental and theoretical investigations on smaller alcohols have been carried out by different groups. Experimental data of the ignition delay times, laminar flame velocities, species profiles for alcohols from C_1–C_4, under a broad range of initial conditions, have been gathered and reorganized in a recent review by Sarathy et al [7]. High-level ab initio calculations on the thermal decomposition reactions of methanol [8], ethanol [9], 2-butanol [10], iso-butanol [11] have been performed, and were found to be in good agreement with the directly measured ones. H-atom abstraction reactions from the alcohol molecule by $\dot{H}$, $\dot{O}H$ and $H\dot{O}_2$ radicals have also been investigated theoretically, for methanol [12-14], ethanol [9, 15] and butanol isomers [16-18]. Comprehensive mechanisms for the oxidation of methanol and ethanol, with simpler structures, have already been comprehensively reviewed by Sarathy et al. [7]. Man et al. [19] modeled the high temperature oxidation of propanol isomers at temperatures over 1100 K, and conducted shock tube ignition delay time measurements in the temperature range of 1100 – 1500 K at pressures from 1.2 – 16 atm. Sarathy et al. [20] proposed a comprehensive chemical kinetic mechanism for the oxidation of butanol isomers, capable of well reproducing experimental measured species profiles in flames and jet-stirred reactors, laminar flame speeds and shock tube ignition delay times, under a wide range of temperatures and pressures.

Recently, larger alcohols have been the focus of many studies due to their higher energy content [21] and n-pentanol with its higher energy value and reactivity is a promising component for diesel blends [22]. It is reported that n-pentanol could improve the cetane number of diesel blends [23] and decrease CO, hydrocarbon, NOx, smoke and particulate emissions [24-27]. Togbé et al. [28] measured speciation of 1-pentanol oxidation in JSR at 10 atm and laminar flame speeds of 1-pentanol at 423 K and 1 atm over equivalence ratios of 0.7–1.4, and developed a chemical kinetic model to represent their experimental data. Dayma et al. [29] modeled the species

profiles of iso-pentanol oxidation against the data obtained in a jet-stirred reactor at 10 atm in the temperature range of 530–1220 K, at equivalence ratios of 0.35–4. Serinyel et al. [30] studied the oxidation of 2-methyl-1-butanol from fuel-lean to fuel-rich mixtures in a jet-stirred reactor at 10 atm, over 700–1200 K, and proposed a mechanism that is also able to predict the ignition delay times and laminar flame speeds of 2-methyl-1-butanol. Theoretical studies have also been performed on the important reaction pathways of pentanol isomers. Van de Vijver et al. [31] computed the pressure- and temperature-dependent rate coefficients for the decomposition and isomerization reaction pathways of 1-pentanol by solving the master equation. Rate constants of the decomposition reactions of 2-pentanol [32], and H-atom abstraction reactions from pentanol isomers by $\dot{O}H$ radical [33] have also been calculated through theoretical approaches. By far, however, investigations on the combustion process of pentan-2-ol oxidation are quite limited in the literature.

Li et al. [34] measured Laminar flame speeds of 1-, 2-, and 3-pentanol isomers with air mixtures at equivalence ratios of 0.6–1.8, with initial pressures of 0.10–0.75 MPa, and initial temperatures of 393–473 K employing the outwardly propagating spherical flame. They found the laminar flame speed of 1-pentanol is the fastest, followed by that of 3- and 2-pentanol isomers and the difference between them decreases when pressure increases. Köhler et al. [35] investigated oxidation of 1-, 2- and 3-pentanol doped hydrogen flat flame employing molecular-beam mass spectrometry, and presented the first comparative flame study for 1-, 2- and 3-pentanol with experimental speciation data and kinetic modeling. Van de Vijver et al. [31] have carried out the theoretical investigations on the potential energy surface for decomposition and isomerization reactions of 1-pentanol radicals at UCCSD(T)-F12a/cc-pVTZ-F12//M06-2X/6-311++G(d,p) level of theory and rate coefficients for the reaction channels of interest have been investigated. Pentan-2-ol radicals can be formed through hydrogen atom abstraction reactions by mainly H, CH_3 and OH, from fuel molecules directly, and their subsequent reactions are important in determining the fuel consumption process under different conditions [31]. It is shown that the decomposition and isomerization reactions of 1-pentanol radicals are of significant importance in describing the fuel conversion and

product selectivity [31]. However, theoretical investigations on the potential energy surface and rate coefficients

calculations on pentan-2-ol radicals have not been reported in the literature so far. Thus, this work aims to carry out

theoretical calculations on the decomposition and isomerization reactions of pentan-2-ol radicals to provide

accurate kinetic data for the model development of pentan-2-ol oxidation which is the part II of this work (in

Supplemental Material).

2. Method

2.1 Potential Energy Surface.

The B2PLYPD3 [36] method with the 6-311++G(d,p) [37] basis set was employed to optimize the geometries of

reactants, intermediates, transition states (TSs), and products for all the species involved in the title reactions.

Zero-point vibrational energy corrections (ZPE) were calculated at the same level of theory. Single-point energies

of all species are determined at the ROCCSD(T) level using the cc-PVQZ and cc-pVTZ [38] which were

extrapolated to the complete basis set limit (CBS) [39]:

$$E_{CBS} = E_{ROCCSD(T)/cc\text{-}pVQZ} + \left(E_{ROCCSD(T)/cc\text{-}pVQZ} - E_{ROCCSD(T)/cc\text{-}pVTZ} \right) * 4^4 / (5^4 - 4^4) \qquad (1)$$

The low frequency torsional modes were treated as hindered rotors with their potential scanned at the

B2PLYPD3/6-311++G(d,p) level of theory. All geometry optimizations and single point energies are performed

with Molpro program [40] and Gaussian 09 [41].

2.2 Rate Constants Calculations.

The Master Equation System Solver (MESS) developed by Klippenstein et al. [42] was used to calculate

temperature and pressure-dependent rate constants over 300–2000 K and 0.01–100 atm. The interaction between

the reactant and N_2 bath gas was modeled employing the Lennard-Jones (L-J) potential [43]. For N_2, $\sigma = 3.6$ Å and

$\varepsilon = 68$ cm^{-1} were used, while for $\dot{C}_5H_{11}O$, $\sigma = 6.269$ Å and $\varepsilon = 341.3$ cm^{-1} were used [44]. A single-parameter

exponential down model with $<\Delta E>_{down} = 200 \times (T/300)^{0.75}$ cm^{-1} was used to represent the collisional energy

transfer function [45]. The calculated rate constants were fitted to a modified Arrhenius expression as a function of temperature $k = AT^n \exp(-E/RT)$.

2.3 Thermochemistry Calculations.

The enthalpies of formation at 0 K for all species are calculated based on atomization approaches, using CBS-APNO[46], CBS-QB3[47], G3[48], and G4[49] composite methods. The 0 K formation enthalpies, vibrational frequencies, rotational constants and 1-D internal rotational potentials are used as input for the MESS code to calculate temperature-dependent partition functions of each species. With the partition functions, we calculated temperature-dependent thermochemical properties of enthalpies, entropies and heat capacities by calling to the ThermP code [50, 51] and converted to NASA polynomial format through PAC99 [50-52].

3 Results and Discussion

3.1 Potential energy surface.

Potential energy surface for the isomerization and β-scission reactions of pentanon-2-ol radicals are shown in Figure 1. The addition reaction between ethyl radical and $CH_2=COHCH_3$ forming pentanol2-2 (W1) is treated as the entrance channel. Joint structure treatments were employed for transition states and intermediates that have more than one stable conformer.
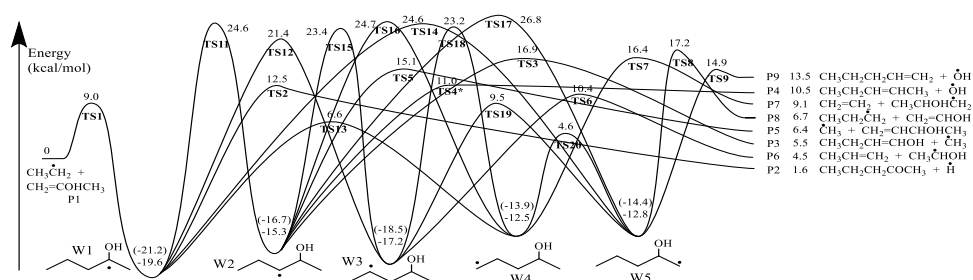

Figure 1. The $\dot{C}_5H_{11}O$ potential energy surface (including ZPE) accessed upon isomerization and decomposition of pentan-2-ol radical. Energies are calculated at the ROCCSD(T)//CBS level of theory (kcal/mol).

3.1.1 Isomerization reactions. The isomerization reaction from pentanol2-2 (W1) to pentanol2-5 (W4) with a barrier of 26.2 kcal/mol is the dominant channel for the consumption of W1, close to the barrier height for

pentanol2-4 (W3) to pentanol2-1 (W5) is 26.7 kcal/mol through a five-membered-ring TS. However, the barrier height for the isomerization process from pentanol2-5 (W4) to pentanol2-1 (W5) is even lower, through a six-membered-ring TS is 17.1 kcal/mol which is much lower. The barrier heights for other isomerization channels are relatively high, which are more than 30 kcal/mol, via three or four-membered-ring TSs. The radical of pentanol2-3 (W2) could not easily isomerize to other four wells because the barrier heights of isomerization reactions are all higher than 38 kcal/mol.

3.1.2 β-scission reactions. The most dominant products formed from pentanol2-2 (W1) are ethyl radical and $CH_2=COHCH_3$ (P1) with a barrier of 28.6 kcal/mol, the formation of 2-pentanone and H (P2) from W1 with a higher barrier height of 32.1 kcal/mol is not competitive. The major products formed from pentanol2-3 (W2) are 2-pentene + OH (P4) with a barrier height of 26.3 kcal/mol. It should be noted that the geometries of reaction with *, pentanol2-3 (W2) to 2-pentene + OH (P4), is calculated by employing BHandHLYP [53] method with the 6-311++G(d,p) basis set, because the transition state could not be located with the B2PLYPD3 method. We use trans structures which have lower energy for 2-pentene in the rate constant calculations. The cis conformer of 2-pentene can also be formed in the decomposition of W2 whose barrier height is 0.8 kcal/mol higher than that in the trans conformer. The barrier heights for the formation of propyl radical + vinyl alcohol (P8) and 1-pentene + OH (P9) pentanol2-1 (W5) are 30.0 and 27.7 kcal/mol respectively with the later reaction channel more competitive. For the decomposition reactions of pentanol2-4 (W3), the formation of propene and CH_3CHOH (P6) is the most favored channel.

3.2 Rate Coefficients

Pressure and temperature dependent rate coefficients have been calculated by using the MESS program [42]. Isomerization and dissociation rate constants and branching ratios for the key reactions discussed above (as a function of temperature at 1 atm) are shown in Figure 2–Figure 6. The calculated rate constants and branching ratios over 300-2000 K and 0.01－100 atm are provided in the Supplemental Material.
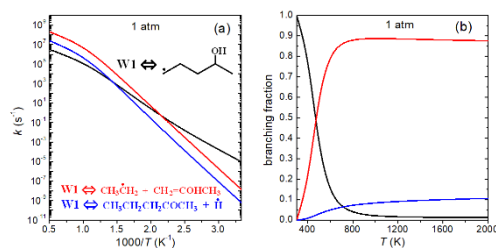
Figure 2 (a) Comparison of rate constants for key reactions from W1 radical and (b) Branching ratios of key products from W1 radical.

3.2.1 Pentanol2-2 (W1) to products. Rate constants for key reactions from W1 radical and branching ratios of key products from W1 radical are shown in Figure 2. The isomerization reaction of pentanol2-2 (W1) to pentanol2-5 (W4) dominate in the temperature range of 300 to 500 K through the pressure range we investigated here and this is consistent with the energy barrier calculation. When temperature is above 500K, the formation of ethyl radical and $CH_2=COHCH_3$ (P1) dominates over the pressures of 0.01-100 atm. Notably, at 0.01 atm and when temperature is above 700K, the branching ratio of pentanol2-1 (W5) is about 5 %, which is higher than the formation of pentanol2-5 (W4). However, when pressure goes up to 1 atm, pentanol2-1 (W5) is only of minor importance.
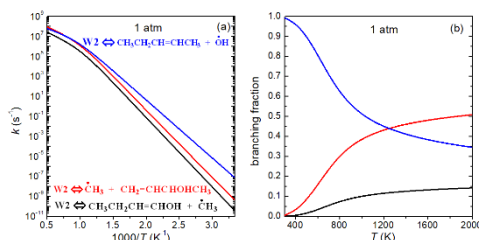

Figure 3 (a) Comparison of rate constants for key reactions from W2 radical and (b) Branching ratios of key products from W2 radical.

3.2.2 Pentanol2-3 (W2) to products. Rate constants for key reactions from W1 radical and branching ratios of key products from W1 radical are shown in Figure 3. As mentioned above, pentanol2-3 (W2) could not easily isomerize to other four wells given the relatively higher barrier height. The major products are hence $CH_3CH_2CH=CHOH + CH_3$ (P3), 2-pentene + OH (P4) and $CH_3 + CH_2=CHCHOHCH_3$ (P5). A strong pressure dependence of the rate constant and branching ratio was observed for those reaction channels. At a lower pressure of 0.01atm, the formation of 2-pentene + OH (P4) dominates the entire temperature range of this work and the branching ratio of

CH$_3$ + CH$_2$=CHCHOHCH$_3$ (P5) is larger than CH$_3$CH$_2$CH=CHOH + CH$_3$ (P3), which is consistent with the barrier height comparison of these three channels. However, when pressure reaches 1 atm and temperature is above 1200K, the formation of CH$_3$ + CH$_2$=CHCHOHCH$_3$ (P5) is much favored than 2-pentene + OH (P4). At 100 atm, the branching fraction of CH$_3$ + CH$_2$=CHCHOHCH$_3$ (P5) is about 60 % at 2000K. The formation of 2-pentene + OH dominates at temperatures below 800 K, and its relative importance declines when pressure and temperature is getting higher.
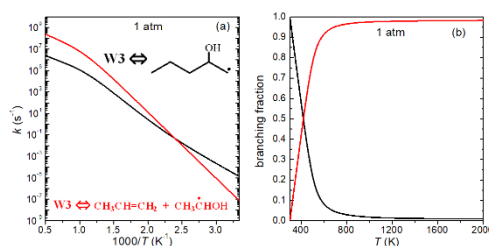

Figure 4 (a) Comparison of rate constants for key reactions from W3 radical and (b) Branching ratios of key products from W3 radical.

3.2.3 Pentanol2-4 (W3) to products. Rate constants for important reactions from W1 radical and branching ratios of important products from W1 radical are shown in Figure 4. There are two dominating products, pentanol2-1 (W5) and propene and CH$_3$CHOH (P6). The branching ratio results do not show strong pressure dependence. Above about 400 K, propene and CH$_3$CHOH (P6) become the most important products.

Figure 5 (a) Comparison of rate constants for key reactions from W4 radical and (b) Branching ratios of key products from W4 radical.

3.2.4 Pentanol2-5 (W4) to products. Rate constants and branching ratio for important reactions started from W1 radical are shown in Figure 5. Rate constant and branching ratio results for the formation of ethylene + CH$_3$CHOHCH$_2$ (P7) also show strong pressure dependence. At 0.01 atm, the formation of pentanol2-1 (W5) is

8

dominant when T < 800K. At 1 atm, the formation of ethyl radical and $CH_2=COHCH_3$ (P1) become dominant in the temperature range of 1300–1800 K. When temperature goes higher than 1800 K, the formation of ethylene + $CH_3CHOHCH_2$ (P7) becomes dominant. When pressure goes up to 100 atm, the formation of ethylene + $CH_3CHOHCH_2$ (P7) becomes dominant when temperature is above 1200 K, and the branching fraction reaches 75 % at 2000K. At lower pressure of 0.01 and 1 atm, the rate constant of pentanol2-5 (W4) to pentanol2-1 (W5) is higher than pentanol2-2 (W1) in the entire temperature range of interest in this work. However, when pressure goes up to 100 atm, rate constants of pentanol2-5 (W4) to pentanol2-1 (W5) and pentanol2-2 (W1) are almost equal when T > 1100 K. Reaction pathways of pentanol2-5 (W4) to form propyl radical + vinyl alcohol (P8) and 1-pentene + OH (P9) are of minor importance, with the relative yields both below 10 %.
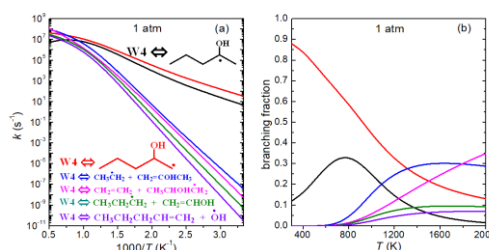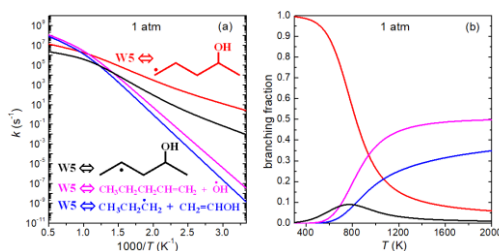

Figure 6 (a) Comparison of rate constants for key reactions from W5 radical and (b) Branching ratios of key products from W5 radical.

3.2.5 Pentanol2-1 (W5) to products. Rate constants for important reactions from W1 radical and branching ratios of important products from W1 radical are shown in Figure 6. At 0.01 atm, the isomerization of pentanol2-1 (W5) to pentanol2-5 (W4) is dominant in the temperature range from 300 to 900 K, which is consistent with the relative barrier height for this reaction process. The formation of pentanol2-2 (W1), ethyl radical and $CH_2=COHCH_3$ (P1), propene and CH_3CHOH (P6), are important at 0.01 atm, and become negligible when pressure is higher than 1 atm over 500 – 2000 K. The formation of propyl radical + vinyl alcohol (P8) become important at 1 and 100 atm, especially when temperature is above 1000 K. At 1 atm, the formation of 1-pentene + OH (P9) is higher than that of propyl radical + vinyl alcohol (P8) over the entire temperature range, which is consistent with the barrier height comparison. However, the branching ratio becomes equal to 47% when temperature reaches 2000 K at 100 atm.

9

When temperature is above 1000 K, branching fraction for the formation of 1-pentene + OH (P9) remains around 50%. However, when pressure reaches 100 atm, the formation of 1-pentene + OH (P9) starts to be overwhelmed by that of propyl radical + vinyl alcohol (P8) with temperature above 1200K.

3.3 Thermochemistry Calculations.

Thermochemistry data of $\Delta H_{f,298}^{\Theta}$, S_{298}^{Θ}, and C_p for the species in this work was calculated and compared with the ones in the literature, shown in Tables 1 and 2. Literature data come from the Active Thermochemical Tables (ATcT) [54], the Third Millennium Ideal Gas and Condensed Phase Thermochemical Database for Combustion [56] (abbreviated as Burcat's database in this paper), and the NIST Chemistry Webbook [55]. It can be seen that most of our calculated results are in good agreement with the literature data except for few cases. Entropy values for C_2H_5 and 2-pentene at 298 K show relatively larger differences with the values in Burcat's database by 2.4 and 6.7 cal/K·mol, respectively. However, the entropy of 2-pentene at 298 K from our calculation is quite close to the value calculated by Power et al. [57] (within 0.1 cal/K·mol) marked as asterisk in Table 1. The entropy of pentan-2-ol at 298 K obtained in this work also differs from the value in Burcat's database by 1.9 cal/K·mol, but it is closer to the value in NIST Chemistry Webbook (within 0.6 cal/K·mol). For the computed heat capacities at 298 K, results for pentan-2-ol, propen-2-ol and 2-pentene display relatively larger discrepancies with the values in Burcat's database (by 2.2, 1.3 and 2 cal/K·mol, respectively). Detailed reasons for this discrepancy between the ab initio calculations carried out in this work and the ones in the literature are unclear.

Table 1. Thermochemistry ($\Delta H_{f,298}^{\Theta}$ and S_{298}^{Θ}) comparison of species on $C_5H_{11}\dot{O}$ PES with literature data.

Species	$\Delta H_{f,298}^{\Theta}$ [kcal mol^{-1}]		S_{298}^{Θ} [cal K^{-1} mol^{-1}]	
	This study	Literature	This study	Literature
Pentan-2-ol	-75.3	-74.7[b], -75±0.3[b], -75.2±0.4[b], 75.7±1.9[c]	94.5	93.7±0.2[b], 92.1[c]
C_2H_5	28.7	28.7±0.1[a], 28.4±0.5[b], 28.6±	60.5	58.1[c]
Propen-2-ol (P12)	-40.3	-39.3±0.3[a], -42.1[b], -38.2±1.9[b], -39.0±1.9[c]	69.7	69.9[c]
2-Pentanone (P21)	-62.3	-61.9±0.3[b]	90.9	
1-Buten-1-ol (P31)	-40.6		81.2	
CH_3	34.6	35.0[a], 34.8[b], 35.1±0.2[b], 35.1[c]	46.5	46.4[b], 46.4[c]
2-Pentene (P41)	-7.1	-7.6±0.5[b], -7.3±1.9[c]	81.8	88.5[c], 81.9*

10

OH	8.9	9.0[a], 9.3[b], 8.9±0.1[c]	43.8	43.9[b], 43.9[c]
3-Buten-2-ol (P52)	-39.5		81.7	
Propene (P61)	5.0	4.8±0.1[a], 4.9[b], 4.9, 4.8±0.1[c]	63.7	63.7[c]
Ethanol-1 (P62)	-13.6	-13.3±0.2 [a], -13.2±0.1 [c]	67.8	69.1[c]
Ethylene (P71)	12.6	12.5[a], 12.5[b], 12.5±0.1[b], 12.5[c]	52.3	52.4[b], 52.4[c]
Isopropyl Alcohol-1 (P72)	-15.3		79.3	
Propane-1 (P81)	24.0	24.1±0.1[a], 23.9±0.5[b], 24.2 ±	70.7	69.4[c]
Ethenol (P82)	-29.5	-29.6±0.2[a], -30.6[b], -29.9±2.0[b], -26.5±2.0 [b], -29.8[c]	62.0	62.4[c]
1-Pentene (P91)	-4.7	-5.3±2.2[b], -5.1[c]	83.3	83.0[c]
Pentanol2-2 (W1)	-32.7		96.1	
Pentanol2-3 (W2)	-27.6		98.2	
Pentanol2-4 (W3)	-30.0		94.5	
Pentanol2-5 (W4)	-25.4		91.5	
Pentanol2-1 (W5)	-25.4		98.3	

[a]Active Thermochemical Tables (Branco Ruscic Argonne National Lab.). [54]

[b]NIST Chemistry Webbook. [55]

[c]Third Millennium Ideal Gas and Condensed Phase Thermochemical Database for Combustion (Burcat). [56]

Table 2. Thermochemistry (C_p) comparison of species on $C_5H_{11}\dot{O}$ PES with literature data.

	$C_p(T)$ [cal K^{-1} mol^{-1}]													
	This Study							Literature						
Species	300	400	500	600	800	1000	1500	300	400	500	600	800	1000	1500
Pentan-2-ol	33.2	40.5	47.5	53.7	63.1	70.3	81.7	31.0[c]						
Pentanol2-2 (W1)	32.9	39.9	46.4	52.1	60.6	67.1	77.3							
Pentanol2-3 (W2)	34.2	40.2	46.1	51.4	59.8	66.4	76.8							
Pentanol2-4 (W3)	32.3	39.4	46.2	52.1	60.9	67.6	78.0							
Pentanol2-5 (W4)	36.1	44.0	50.2	55.3	63.1	69.0	78.7							
Pentanol2-1 (W5)	33.8	40.6	46.8	52.3	60.7	67.1	77.2							
C2H5 (P11)	12.1	14.5	16.9	19.1	22.6	25.4	29.9	12.1[c]						
Propen-2-ol (P12)	20.5	25.1	28.9	31.9	36.3	39.7	45.1	19.2[c]						
2-Pentanone (P21)	28.6	35.3	41.7	47.3	56.0	62.6	72.9	28.5[b]	36.4	42.6				
1-Buten-1-ol (P31)	24.3	30.0	35.2	39.7	46.2	51.1	58.9							
CH3 (P32)	9.4	10.1	10.8	11.5	12.8	13.9	16.1	9.3[b]	10.1	10.8	11.5	12.9	14.1	16.3
								9.2[c]						
2-Pentene (P41)	26.0	32.1	38.0	43.3	51.6	58.0	68.0	26.1[b]	32.6	38.7	44.0	52.6	59.0	68.9
								24.0[c]						
OH (P42)	7.2	7.1	7.0	7.0	7.1	7.2	7.7	7.2[b]	7.1	7.1	7.1	7.2	7.3	7.9
								7.1[c]						
3-Buten-2-ol (P52)	27.4	32.9	37.4	41.1	47.0	51.6	59.1							
Propene (P61)	15.1	18.7	22.2	25.3	30.2	34.0	39.9	15.4[b]	19.2	22.7	25.8	30.8	34.5	40.4
								15.5[b]	19.2	22.6				
								15.4[c]						
Ethanol-1 (P62)	15.7	18.6	21.4	23.8	27.7	30.6	35.4	15.3[c]						
Ethylene (P71)	10.2	12.4	14.7	16.7	19.7	22.1	26.0	10.3[b]	12.7	14.9	16.9	20.1	22.4	26.3
								10.4[b]	12.6	15.2				
								10.3[b]	12.7	14.9	16.9	20.0	22.4	26.3
								10.3[c]						
Isopropyl Alcohol-1(P72)	22.3	26.5	30.3	33.5	38.6	42.4	48.8							

Propane-1 (P81)	17.1	21.1	24.9	28.2	33.4	37.5	44.0	17.0[c]						
Ethenol (P82)	15.0	18.0	20.5	22.5	25.4	27.5	31.0	14.9[c]						
1-Pentene (P91)	26.0	32.4	38.5	43.9	52.0	58.4	68.2	26.0[b]	32.9	39.2	44.5	52.8	58.8	68.2
								25.9[c]						

4 Conclusion

Theoretical rate constants and thermochemistry investigations on pyrolysis of pentan-2-ol radicals have been carried out in this work. According to the barrier height for bimolecular products, ethyl radical and CH_2=COHCH$_3$ (P1), 2-pentene + OH (P4) and 1-pentene + OH (P9) are found to be the more favorable products from different isomers.

Strong pressure and temperature dependence has been shown in the rate constants calculations for the title reactions. The formation of 2-pentene + OH (P4) is dominant at temperatures below 800 K and pressures below 10 atm. However, as pressure increases, the dominant zone of the formation of 1-pentene + OH (P9) shifts to higher temperatures. Thermochemistry data for the species involved in this work has been calculated and compared with the ones in the literature. Most of our results show good agreement with literature data, except for some species such as 2-pentene, pentan-2-ol and propen-2-ol, the reason of it is unclear so far. This work provides new kinetics and thermodynamics data for decomposition and isomerization reactions of pentan-2-ol radicals which was used in the model development for pentan-2-ol oxidation (part II of this work).

Reference

[1] A.K. Agarwal, Biofuels (alcohols and biodiesel) applications as fuels for internal combustion engines, Progress in Energy and Combustion Science, 33 (2007) 233-271.

[2] G. Black, H.J. Curran, S. Pichon, J.M. Simmie, V. Zhukov, Bio-butanol: Combustion properties and detailed chemical kinetic model, Combustion and Flame, 157 (2010) 363-373.

[3] M. Gautam, D.W. Martin, Combustion characteristics of higher-alcohol/gasoline blends, Proceedings of the Institution of Mechanical Engineers, Part A: Journal of Power and Energy, 214 (2005) 497-511.

[4] G.P. Robertson, S.K. Hamilton, B.L. Barham, B.E. Dale, R.C. Izaurralde, R.D. Jackson, D.A. Landis, S.M. Swinton, K.D. Thelen, J.M. Tiedje, Cellulosic biofuel contributions to a sustainable energy future: Choices and outcomes, Science, 356 (2017).

[5] J.M. Bergthorson, M.J. Thomson, A review of the combustion and emissions properties of advanced transportation biofuels and their impact on existing and future engines, Renewable and Sustainable Energy Reviews, 42 (2015) 1393-1417.

[6] K. Kohse-Hoinghaus, P. Osswald, T.A. Cool, T. Kasper, N. Hansen, F. Qi, C.K. Westbrook, P.R. Westmoreland, Biofuel combustion chemistry: from ethanol to biodiesel, Angew Chem Int Ed Engl, 49 (2010) 3572-3597.

[7] S.M. Sarathy, P. Oßwald, N. Hansen, K. Kohse-Höinghaus, Alcohol combustion chemistry, Prog. Energy Combust. Sci., 44 (2014) 40-102.

[8] A.W. Jasper, S.J. Klippenstein, L.B. Harding, B. Ruscic, Kinetics of the reaction of methyl radical with hydroxyl radical and methanol decomposition, J. Phys. Chem. A, 111 (2007) 3932-3950.

[9] R. Sivaramakrishnan, M.-C. Su, J. Michael, S. Klippenstein, L. Harding, B. Ruscic, Rate constants for the thermal decomposition of ethanol and its bimolecular reactions with OH and D: reflected shock tube and theoretical studies, J. Phys. Chem. A, 114 (2010) 9425-9439.

[10] A.M. El-Nahas, A.H. Mangood, H. Takeuchi, T. Taketsugu, Thermal decomposition of 2-butanol as a potential nonfossil fuel: a computational study, J. Phys. Chem. A, 115 (2011) 2837-2846.

[11] C.-W. Zhou, S.J. Klippenstein, J.M. Simmie, H.J. Curran, Theoretical kinetics for the decomposition of iso-butanol and related (CH3) 2ĊH+ ĊH2OH reactions, Proc. Combust. Inst., 34 (2013) 501-509.

[12] R. Meana-Pañeda, D.G. Truhlar, A. Fernández-Ramos, High-level direct-dynamics variational transition state theory calculations including multidimensional tunneling of the thermal rate constants, branching ratios, and kinetic isotope effects of the hydrogen abstraction reactions from methanol by atomic hydrogen, J. Chem. Phys., 134 (2011) 094302.

[13] S. Xu, M. Lin, Theoretical study on the kinetics for OH reactions with CH3OH and C2H5OH, Proc. Combust. Inst., 31 (2007) 159-166.

[14] S.J. Klippenstein, L.B. Harding, M.J. Davis, A.S. Tomlin, R.T. Skodje, Uncertainty driven theoretical kinetics studies for CH3OH ignition: HO2+ CH3OH and O2+ CH3OH, Proc. Combust. Inst., 33 (2011) 351-357.

[15] J. Zheng, D.G. Truhlar, Multi-path variational transition state theory for chemical reaction rates of complex polyatomic species: ethanol+ OH reactions, Faraday Discuss., 157 (2012) 59-88.

[16] P. Seal, G. Oyedepo, D.G. Truhlar, Kinetics of the hydrogen atom abstraction reactions from 1-butanol by hydroxyl radical: theory matches experiment and more, J. Phys. Chem. A, 117 (2013) 275-282.

[17] C.W. Zhou, J.M. Simmie, H.J. Curran, Rate constants for hydrogen abstraction by HȮ2 from n-butanol, Int. J. Chem. Kinet., 44 (2012) 155-164.

[18] C.-W. Zhou, J.M. Simmie, H.J. Curran, Rate constants for hydrogen-abstraction by Ȯ H from n-butanol, Combust. Flame, 158 (2011) 726-731.

[19] X. Man, C. Tang, J. Zhang, Y. Zhang, L. Pan, Z. Huang, C.K. Law, An experimental and kinetic modeling study of n-propanol and i-propanol ignition at high temperatures, Combustion and Flame, 161 (2014) 644-656.

[20] S.M. Sarathy, S. Vranckx, K. Yasunaga, M. Mehl, P. Oßwald, W.K. Metcalfe, C.K. Westbrook, W.J. Pitz, K. Kohse-Höinghaus, R.X. Fernandes, A comprehensive chemical kinetic combustion model for the four butanol isomers, Combust. Flame, 159 (2012) 2028-2055.

[21] C. Tang, L. Wei, X. Man, J. Zhang, Z. Huang, C.K. Law, High temperature ignition delay times of C5 primary alcohols, Combustion and Flame, 160 (2013) 520-529.

[22] J. Campos-Fernandez, J.M. Arnal, J. Gomez, N. Lacalle, M.P. Dorado, Performance tests of a diesel engine fueled with pentanol/diesel fuel blends, Fuel, 107 (2013) 866-872.

[23] H.K. Imdadul, H.H. Masjuki, M.A. Kalam, N.W.M. Zulkifli, A. Alabdulkarem, M.M. Rashed, A.M. Ashraful, Influences of ignition improver additive on ternary (diesel-biodiesel-higher alcohol) blends thermal stability and diesel engine performance, Energy Conversion and Management, 123 (2016) 252-264.

[24] B. Rajesh Kumar, S. Saravanan, D. Rana, A. Nagendran, Combined effect of injection timing and exhaust gas recirculation (EGR) on performance and emissions of a DI diesel engine fuelled with next-generation advanced biofuel – diesel blends using response surface methodology, Energy Conversion and Management, 123 (2016) 470-486.

[25] L. Wei, C.S. Cheung, Z. Huang, Effect of n-pentanol addition on the combustion, performance and emission characteristics of a direct-injection diesel engine, Energy, 70 (2014) 172-180.

[26] Z.-H. Zhang, S.-M. Chua, R. Balasubramanian, Comparative evaluation of the effect of butanol–diesel and pentanol–diesel blends on carbonaceous particulate composition and particle number emissions from a diesel engine, Fuel, 176 (2016) 40-47.

[27] L. Li, J. Wang, Z. Wang, J. Xiao, Combustion and emission characteristics of diesel engine fueled with diesel/biodiesel/pentanol fuel blends, Fuel, 156 (2015) 211-218.

[28] C. Togbé, F. Halter, F. Foucher, C. Mounaim-Rousselle, P. Dagaut, Experimental and detailed kinetic modeling study of 1-pentanol oxidation in a JSR and combustion in a bomb, Proceedings of the Combustion Institute, 33 (2011) 367-374.

[29] G. Dayma, C. Togbé, P. Dagaut, Experimental and Detailed Kinetic Modeling Study of Isoamyl Alcohol (Isopentanol) Oxidation in a Jet-Stirred Reactor at Elevated Pressure, Energy & Fuels, 25 (2011) 4986-4998.

[30] Z. Serinyel, C. Togbé, G. Dayma, P. Dagaut, An experimental and modeling study of 2-methyl-1-butanol oxidation in a jet-stirred reactor, Combustion and Flame, 161 (2014) 3003-3013.

[31] R. Van de Vijver, K.M. Van Geem, G.B. Marin, J. Zádor, Decomposition and isomerization of 1-pentanol radicals and the pyrolysis of 1-pentanol, Combustion and Flame, 196 (2018) 500-514.

[32] A. Parandaman, B. Rajakumar, Thermal Decomposition of 2-Pentanol: A Shock Tube Study and RRKM Calculations, J. Phys. Chem. A, 120 (2016) 8024-8036.

[33] B. Aazaad, S. Lakshmipathi, Reaction of Pentanol isomers with OH radical–A theoretical perspective, Mol. Phys., 116 (2018) 1153-1165.

[34] Q. Li, E. Hu, X. Zhang, Y. Cheng, Z. Huang, Laminar Flame Speeds and Flame Instabilities of Pentanol Isomer–Air Mixtures at Elevated Temperatures and Pressures, Energy & Fuels, 27 (2013) 1141-1150.

[35] M. Köhler, T. Kathrotia, P. Oßwald, M.L. Fischer-Tammer, K. Moshammer, U. Riedel, 1-, 2- and 3-Pentanol combustion in laminar hydrogen flames – A comparative experimental and modeling study, Combustion and Flame, 162 (2015) 3197-3209.

[36] S. Grimme, Semiempirical hybrid density functional with perturbative second-order correlation, J Chem Phys, 124 (2006) 034108.

[37] A.D. McLean, G.S. Chandler, Contracted Gaussian basis sets for molecular calculations. I. Second row atoms, Z=11–18, The Journal of Chemical Physics, 72 (1980) 5639-5648.

[38] T.H. Dunning, Gaussian basis sets for use in correlated molecular calculations. I. The atoms boron through neon and hydrogen, The Journal of Chemical Physics, 90 (1989) 1007-1023.

[39] J.M.L. Martin, Ab Initio Total Atomization Energies of Small Molecules --Towards the Basis Set Limit. , Chem. Phys. Lett., 259 (1996) 10.

[40] A.B. R. D. Amos, A. Berning, P. Celani, D. L. Cooper, M. J. O. Deegan, A. J. Dobbyn, F. Eckert, C. Hampel, G. Hetzer, P. J. Knowles, T. Korona, R. Lindh, A. W. Lloyd, S. J. McNicholas, F. R. Manby, W. Meyer, M. E. Mura, A. Nicklass, P. Palmieri, R. Pitzer, G. Rauhut, M. Schü tz, U. Schumann, H. Stoll, A. J. Stone, R. Tarroni, T. Thorsteinsson and H.-J. Werner, MOLPRO, a package of ab initio programs designed by H.-J. Werner and P. J. Knowles, (2015).

[41] J. Foresman, J.C. Ortiz, J, D. Fox, Gaussian 09, Revision D. 01; Gaussian, Inc.: Wallingford, CT,, (2009).

[42] J.A. Miller, S.J. Klippenstein, Master equation methods in gas phase chemical kinetics, J Phys Chem A, 110 (2006) 10528-10544.

[43] M.J. Pilling, S.H. Robertson, Master equation models for chemical reactions of importance in combustion, Annu Rev Phys Chem, 54 (2003) 245-275.

[44] F.M. Mourits, F.H.A. Rummens, A critical evaluation of Lennard-Jones and Stockmayer potential parameters and of some correlation methods, Can. J. Chem., 55 (1977) 3007-3020.

[45] S.J. Klippenstein, J.A. Miller, The addition of hydrogen atoms to diacetylene and the heats of formation of i-C4H3 and n-C4H3, J Phys Chem A, 109 (2005) 4285-4295.

[46] J.W. Ochterski, G.A. Petersson, J.A. Montgomery, A complete basis set model chemistry. V. Extensions to six or more heavy atoms, The Journal of Chemical Physics, 104 (1996) 2598-2619.

[47] J.A. Montgomery, M.J. Frisch, J.W. Ochterski, G.A. Petersson, A complete basis set model chemistry. VII. Use of the minimum population localization method, The Journal of Chemical Physics, 112 (2000) 6532-6542.

[48] L.A. Curtiss, K. Raghavachari, P.C. Redfern, V. Rassolov, J.A. Pople, Gaussian-3 (G3) theory for molecules containing first and second-row atoms, The Journal of Chemical Physics, 109 (1998) 7764-7776.

[49] L.A. Curtiss, P.C. Redfern, K. Raghavachari, Gaussian-4 theory, J Chem Phys, 126 (2007) 084108.

[50] M. Keçeli, S.N. Elliott, Y.-P. Li, M.S. Johnson, C. Cavallotti, Y. Georgievskii, W.H. Green, M. Pelucchi, J.M. Wozniak, A.W. Jasper, S.J. Klippenstein, Automated computational thermochemistry for butane oxidation: A prelude to predictive automated combustion kinetics, Proceedings of the Combustion Institute, 37 (2019) 363-371.

[51] S.J.K. Murat Keceli, B.J. McBride, S. Gordon, *Quantum Thermochemistry Calculator (Qtc)*, 2018

[52] B.J. McBride, S. Gordon, *Computer Program for Calculating and Fitting Thermodynamic Functions*, 1992

[53] A.D. Becke, A new mixing of Hartree–Fock and local density-functional theories, The Journal of Chemical Physics, 98 (1993) 1372-1377.

[54] B. Ruscic, D. Bross, *Active Thermochemical Tables (ATcT) values based on ver. 1.122d of the Thermochemical Network*, 2018

[55] E. Lemmon, M. McLinden, D. Friend, P. Linstrom, W. Mallard, *NIST Chemistry Webbook, NIST Standard Reference Database Number 69*, National Institute of Standards and Technology: Gaithersburg, 2011

[56] A. Burcat, B. Ruscic, *Third Millennium Ideal Gas and Condensed Phase Thermochemical Database for Combustion (with Update from Active Thermochemical Tables)*, Argonne National Labarotary (ANL): Argonne, IL (United States), 2005

[57] J. Power, K.P. Somers, C.W. Zhou, S. Peukert, H.J. Curran, Theoretical, Experimental, and Modeling Study of the Reaction of Hydrogen Atoms with 1- and 2-Pentene, J Phys Chem A, 123 (2019) 8506-8526.

List of supplemental materials

The rate constants and branching ratio over all pressures of pentan-2-ol.docx

The rate constants and branching ratio over all pressures interested in this work.

Glossary.docx

Code, name and structure of species on $C_5H_{11}\dot{O}$ PES.

ANE-HPL.chem

Modified Arrhenius expressions for the high pressure limit rate constants of the important reaction pathways of pentan-2-ol.

ANE-pressure-dependent.chem

Modified Arrhenius expressions for the pressure-dependent rate constants of the important reaction pathways of pentan-2-ol.

MESS_input_pentan-2-ol.inp

MESS input file for entire reaction pathways of pentan-2-ol in this work.

ThermLst.dat

Enthalpy of formation, Entropy at 298K and Heat Capacities over 300-1500K of species on $C_5H_{11}\dot{O}$ PES.

NASA.dat

Thermodynamic data using the new NASA (9-coefficients) polynomial format of species on $C_5H_{11}\dot{O}$ PES.